

313

**Institut  
de Physique  
Nucléaire  
de Lyon**

Université Claude Bernard

IN2P3 - CNRS



Sw 9803

**LYCEN 9740**  
**CMS CR 1997-015**  
September 1997

Heavy ion physics at LHC with CMS detector

R. Kvatadze<sup>a)</sup>, CMS collaboration

<sup>a)</sup> High Energy Physics Institute, Tbilisi State University, Georgia

---

*Presented at International Europhysics Conference on High Energy Physics, Jerusalem,  
Israel, August 19-26, 1997*

---

# CMS Conference Report

---

July 20, 1997

## Heavy Ion Physics at LHC with CMS Detector

R. Kvatadze<sup>a)</sup>*Institut de Physique Nucléaire de Lyon, France**CMS collaboration*

### Abstract

The CMS (Compact Muon Solenoid) is a general purpose detector, optimised for  $pp$  collisions at LHC. However, a very good muon system, fine granularity and excellent energy resolution of electromagnetic and hadron calorimeters and high quality central tracker gives the possibility of using the detector for specific heavy ion studies.

Various ways of searching for the phase transition from hadronic matter to the plasma of deconfined quarks and gluons in heavy ion collisions with CMS detector have been investigated:

- Production of  $(c\bar{c})$  and  $(b\bar{b})$  resonance states through their muon decay channel to study the colour-screening effect. The dimuon mass spectra and rates of heavy quark bound state production in  $Pb - Pb$  collisions for two weeks of running time are presented. Expected statistics will be sufficient to perform the  $\Upsilon$  family suppression study. Acceptance for  $J/\psi$  detection is mostly concentrated in the forward region.  $Z$  production and its subsequent  $\mu^+\mu^-$  decay can be detected with high statistics and low background ( $\simeq 4\%$ ).
- To study energy losses of a hard parton in QGP (jet quenching) three different processes have been considered: QCD jet pair,  $Z$ +jet and  $\gamma$ +jet production. The possibility of jet recognition in central  $Pb - Pb$  collisions has been investigated. For transverse energy jets  $E_T \geq 50$  GeV the recognition efficiency is close to 100%.

Presented at

*International Europhysics Conference on High Energy Physics, Jerusalem, Israel, August 19-26, 1997*

---

<sup>a)</sup> On leave from High Energy Physics Institute, Tbilisi State University, Georgia.

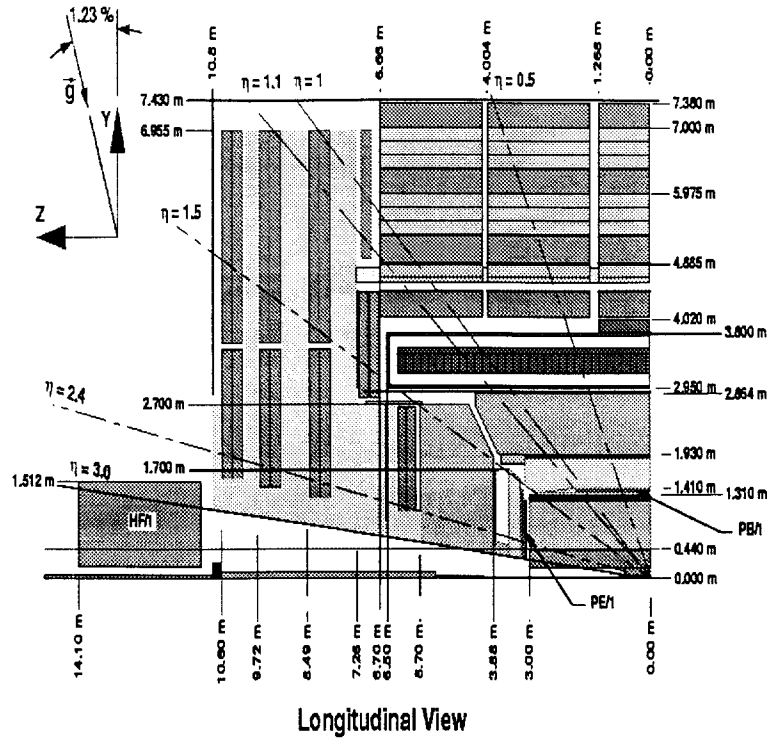


Figure 1: Longitudinal view of CMS detector.

## 1 Introduction

The main motivation for heavy ion experiments at LHC is to study strong interaction thermodynamics and phase transition from hadronic matter to the plasma of deconfined quarks and gluons (QGP). For heavy nuclei  $A \sim 200$  colliding at the center of mass energies of about 5.5 TeV/nucleon, the energy density in central nucleus-nucleus collisions should be well above the expected phase transition value, thus allowing one to probe QGP in asymptotically free ideal gas form [1, 2].

Several measurable effects have been suggested in order to establish the formation of QGP and investigate its properties [2, 3, 4, 5]. Among the proposed probes heavy quarkonium ( $c\bar{c}$ ), ( $b\bar{b}$ ) and high transverse momentum parton (jet) production are especially promising, because they are produced at the early stage of the collision process and carry out information about the evolution of produced system.

The CMS detector with its high quality central tracker, large acceptance muon system, and fine granularity and large geometrical coverage of calorimeters is suitable for these studies.

In the following section a short description of the CMS detector is presented. General conditions for  $Pb-Pb$  collisions at LHC and impact parameter measurement are discussed in section 3. Heavy quark bound states production and their subsequent  $\mu^+\mu^-$  decays are considered in section 4, together with high mass dimuons from Drell-Yan, Z boson and open heavy flavours production. Possibility of jet recognition and production rates for central  $Pb-Pb$  collisions are studied in section 5. Some conclusions are drawn in section 6.

## 2 The CMS detector

Figure 1 shows a schematic longitudinal view of the CMS detector. The central element of CMS is a 13 m long and 6 m diameter solenoid generating a uniform magnetic field of 4 T [6]. The inner part of the detector is occupied by a 6 m long and 1.3 m radius central tracker. The barrel part of the tracker consists of two layers of pixel detectors, four layers of microstrip Si detectors and seven layers of microstrip gas chambers (MSGC). The total number of detection channels in the central tracker is  $\approx 9 \times 10^7$ .

The hadron and electromagnetic calorimeters are located in the coil. The electromagnetic calorimeter is made of high resolution lead-tungstate ( $PbWO_4$ ) crystals. In the barrel part the crystals are  $25\chi_0$  deep with granularity  $\Delta\eta \times \Delta\phi = 0.0145 \times 0.0145$ . The total number of crystals is about  $1.1 \times 10^5$ . The hadron calorimeter consists

of copper absorber plates interleaved with scintillator tiles read-out from embedded wavelength shifting fibres. Segmentation in the barrel is  $\Delta\eta \times \Delta\phi = 0.087 \times 0.087$ . The expected energy resolution for electromagnetic and hadron calorimeters are  $\sigma_E/E = 2.0\%/\sqrt{E} \oplus 0.5\%$  and  $\sigma_E/E = 65.0\%/\sqrt{E} \oplus 5.0\%$  respectively. Electromagnetic and hadron calorimeters extend up to pseudorapidity 3.0 and are complemented in the region  $3.0 \leq |\eta| \leq 5.0$  by quartz-fibre very forward calorimeters.

The CMS muon stations consist of drift tube planes in the barrel and cathode strip chambers in the endcaps, and also include the resistive plate chamber triggering planes with time resolution  $\sim 2$  nsec.

### 3 General conditions for $Pb - Pb$ collisions and impact parameter measurement

At LHC ions will be accelerated up to the energies  $E = E_p \times (2Z/A)$  per nucleon pair, where  $E_p = 7$  TeV is the proton beam energy for LHC. In the case of  $Pb$  nuclei the energy per nucleon pair will be 5.5 TeV and expected average luminosity for a single experiment is  $L \approx 1.0 \times 10^{27} \text{ cm}^{-2}\text{s}^{-1}$ . For the lighter ion beams the luminosity can be much higher e.g. the ratio of luminosities  $L_{Ca}/L_{Pb} \approx 2500$ . The interaction cross-section for  $Pb - Pb$  collisions is about 7.5 b, which leads to the event rate of 7.5 kHz.

For the study of global characteristics like total and transverse energy flow, dependence of the number of secondary particles on the impact parameter ( $b$ ) in nucleus-nucleus collisions the HIJING event generator was used [7].

To investigate the detection possibility of hard processes a different strategy has been exploited. The production cross-sections of hard processes in minimum bias nucleus-nucleus collisions were extrapolated from that in  $pp$  interactions according the parametrization  $\sigma_{AA} = A^{2\alpha} \times \sigma_{pp}$ , with  $\alpha = 0.9$  for ( $J/\psi$ ,  $\psi'$ ),  $\alpha = 0.95$  for ( $\Upsilon$ ,  $\Upsilon'$ ,  $\Upsilon''$ ) states, and  $\alpha = 1.0$  for other hard processes. The cross-sections in  $pp$  collisions were evaluated using the PYTHIA Monte-Carlo program [8], with the default structure functions CTEQ2L and the  $k$ -factor equal to 1. This approach does not take into account the effects of the deflection of the parton structure functions in a nucleus relative to a free nucleon and energy losses of hard partons in dense media.

To estimate the influence of the soft secondary particles, hard process events (generated with PYTHIA program) were superimposed on the "thermal" background. The important parameters for this study are: the multiplicity of "thermal" particles and their transverse momentum distribution (especially high  $P_T$  tail of the spectra). For the number of charged particles emitted per unit of rapidity in the central  $Pb - Pb$  collisions with  $b = 0$  fm we have assumed  $(dN/dy)_{y=0} = 8000$ , according to the HIJING event generator. For the transverse momentum distributions of secondary particles several parametrizations obtained from HIJING, PYTHIA and SHAKER [9] programs were used. The  $\eta$  spectra were described by the sum of two Gaussian functions with the parameters extracted from HIJING event generator.

Figure 2 presents the expected dependence of the detected transverse energy on the impact parameter of  $Pb - Pb$  collisions for barrel, endcap and very forward parts of the CMS calorimeters. The thresholds on cell energy for electromagnetic, hadron and very forward calorimeters were 0.1, 0.5 and 1.0 GeV respectively. Detected transverse energy is strongly increased with decreasing of impact parameter, thus allowing to measure the centrality of the collision and select central  $Pb - Pb$  interaction events with the  $E_T$  trigger. The same dependence was found for lighter ions ( $O$ ,  $Ca$  and  $Nb$ ). About 80% of generated transverse energy will be detected by the CMS calorimeters in central  $Pb - Pb$  collisions.

### 4 Dimuon detection in $Pb - Pb$ collisions

One of the most interesting measurements in heavy ion collisions at LHC will be investigation of heavy quark resonances ( $J/\psi$ ,  $\psi'$ ,  $\Upsilon$ ,  $\Upsilon'$ ,  $\Upsilon''$ ) production. CMS detector with its large acceptance muon system  $|\eta| \leq 2.4$  gives unique possibility to study production of these resonances via dimuon decay channel. Another important feature of the detector is excellent mass resolution ( $\sigma_M \approx 40$  MeV at  $\Upsilon$  mass) which makes possible to distinguish different states of  $\Upsilon$  family.

According to calculations [10] and to the Fermilab results [11] extrapolated to LHC energies and to  $Pb - Pb$  collisions, we have assumed the following value of  $\sigma \times BR(J/\psi \rightarrow \mu^+ \mu^-) = 140$  mb for  $J/\psi$  state production. For the  $\Upsilon$  family we used respectively  $\Upsilon: \Upsilon': \Upsilon'' = 410: 120: 41 \mu\text{b}$ . The resonances were generated in  $(P_T, \eta)$  space according to the distributions given by PYTHIA event generator except for  $P_T$  distribution of  $\Upsilon$  state, which was extracted from the CDF experimental data [11]. The resonances were accepted if both decay muons cross any

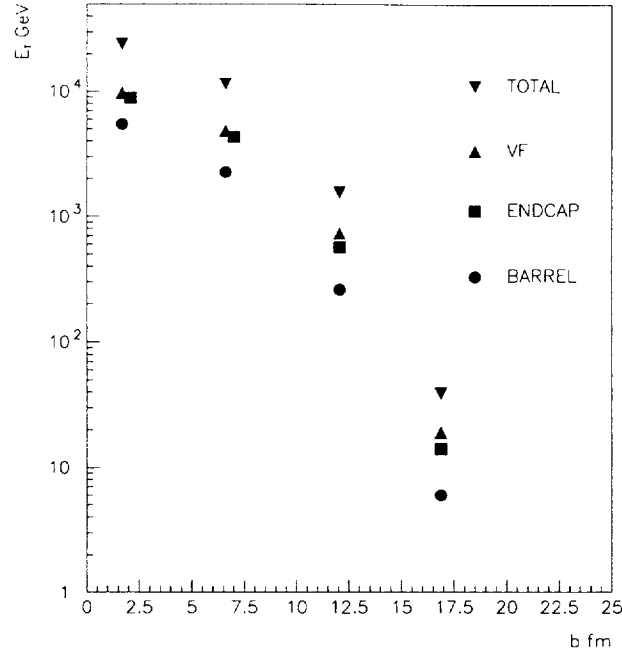


Figure 2: Expected dependence of the detected transverse energy on the impact parameter of  $Pb - Pb$  collisions.

Table 1: Efficiencies and purities for dimuons coming from  $\Upsilon$  and  $\pi/K$  decays for different multiplicity of charged particles.

$(dN/dy)_{y=0}$	8000		2500	
Dimuon origin	$\Upsilon$	$\pi/K$	$\Upsilon$	$\pi/K$
Efficiency, %	66	11	88	16
Purity, %	97		99	

of the muon stations. The dependence of  $\Upsilon$  state acceptance on its transverse momentum is rather flat in both parts of the detector: barrel ( $|\eta| < 1.3$ ) and endcaps ( $1.3 \leq |\eta| \leq 2.4$ ). The acceptance for the  $J/\psi$  state is strongly suppressed in the barrel part for  $P_T < 5$  GeV/c, which is related with the relatively low mass of this resonance. The minimum transverse momentum of  $\mu$  needed to reach the first muon station is about 3 GeV/c at  $\eta = 0$ . Therefore low transverse momentum  $J/\psi$  detection is concentrated only in endcap part. The integrated acceptances for full CMS detector are 7% and 39% for  $J/\psi$  and  $\Upsilon$  states respectively.

Important feature of this study is to suppress muons from the  $\pi$  and  $K$  decays. The first stage of suppression comes from detector design and is connected with the fact that muon chambers are preceded by  $10\chi_I$  material in the barrel part (closest absorber – electromagnetic calorimeter – is at 1.3 m away from the interaction region). The probability that a pion with  $P_T > 3$  GeV/c decays into a detected muon is of the order of  $5 \times 10^{-5}$ . However, this rejection is not enough and at the second stage, a dimuon reconstruction algorithm was used for further reduction of the background. This algorithm [12] together with the information from muon chambers (at least two hits in the first muon station) uses 6 points of measurement: 2 hits in pixel and 4 hits in the outermost MSGC layers of the central tracker. The dimuons from resonance decays were superimposed on “thermal” particle background. Several sets of multiplicity of the secondary particles were used in the analyses. After digitization and clusterization, the tracks have been chosen within  $(\Delta\Phi, \Delta P_T)$  roads and submitted to helix fit. At the end of the algorithm a vertex constraint was applied to the opposite sign pair of candidate tracks. This selection rejects mostly background pairs. Table 1 presents reconstruction efficiencies and purities for dimuons originated from  $\Upsilon$  and  $\pi/K$  decays in the pseudorapidity range  $|\eta| \leq 0.8$  for two different multiplicity of the charged particles. The efficiency to reconstruct dimuon from  $\Upsilon$  decay is 66% for most central  $Pb - Pb$  collisions (8000 charged particle per unit of rapidity) and increasing to 88% for  $(dN/dy)_{y=0} = 2500$ . In both cases the purity is larger than 95%.

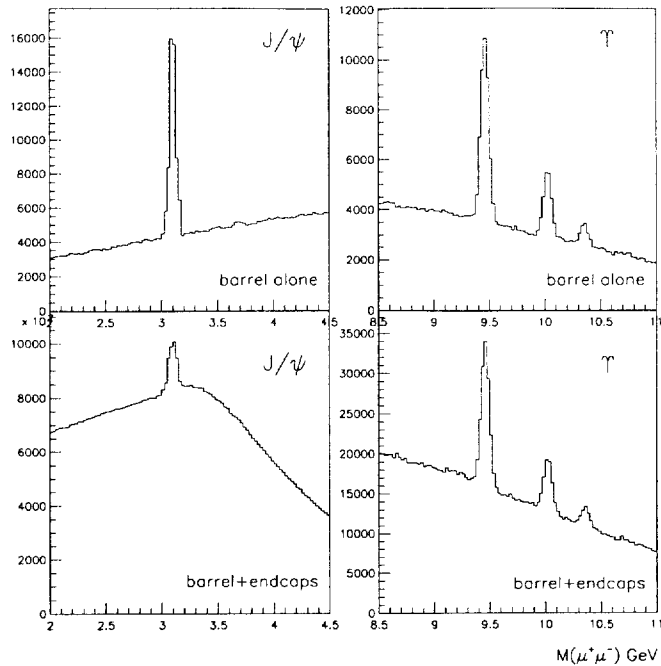


Figure 3: Dimuon mass spectra for  $J/\psi$  and  $\Upsilon$  mass regions in different parts of detector.

Table 2: Expected statistics and signal/background ratios for  $J/\psi$  and  $\Upsilon$  resonances in  $Pb - Pb$  collisions for two weeks of running time ( $1.3 \times 10^6$  s).

Detector	Full CMS			Barrel		
	$J/\psi$	$\Upsilon$	$\Upsilon'$	$J/\psi$	$\Upsilon$	$\Upsilon'$
Statistics	580000	55000	20000	31000	23000	8300
$S/B$	0.17	0.8		1.8	1.6	
$S/\sqrt{S+B}$	290	150		140	120	

Figure 3 shows dimuon mass distribution for  $J/\psi$  and  $\Upsilon$  mass regions in minimum bias  $Pb - Pb$  collisions for barrel and full detector. The used reconstruction efficiencies for resonance states were lower from those shown in table 1 (60% instead of 88% for  $(dN/dy)_{y=0} = 2500$ ) because at that moment less refined algorithm was considered for dimuon reconstruction. The main contribution to the background under the  $\Upsilon$  state is uncorrelated muon pairs from  $\pi/K$  decays, 76% in the barrel part. Contribution of mixed origin dimuons – one muon from hadron decay and another from  $b\bar{b}$  fragmentation is  $\approx 17\%$ . As the background is essentially uncorrelated dimuons it will be possible to subtract it using like-sign muon pairs spectra.

Expected numbers of heavy quark bound states in  $Pb - Pb$  collisions for two weeks of running time detected in different parts of the detector are presented in table 2 together with the signal/background ratios [13]. For  $J/\psi$  state the  $S/B$  ratio in full CMS detector is rather low 0.17. Therefore study of this state will be limited to the barrel part where only  $J/\psi$ 's with  $P_T > 5$  GeV/c can be detected. For  $\Upsilon$  state signal/background ratio ranges from 0.8 in the full detector to 1.6 for barrel part only. Expected statistics will be enough to study correlations between the  $\Upsilon$  production cross-section and its transverse momentum or centrality of the events. It should be mentioned that for lighter ions  $S/B$  ratio for  $\Upsilon$  is much larger, for example in  $Ca - Ca$  collisions this ratio is about 14 for the full detector and  $\approx 23$  for the barrel part.

In the high invariant mass region  $M(\mu^+\mu^-) \geq 20$  GeV main sources of dimuons are Drell-Yan and Z boson production and semileptonic decays of open heavy flavours ( $c\bar{c}$ ,  $b\bar{b}$ ). Figure 4 presents  $\mu^+\mu^-$  pair invariant mass distribution for muons with  $P_T > 5$  GeV/c. A clear signal from  $Z \rightarrow \mu^+\mu^-$  decays is seen. The expected number of detected Z decays in  $\pm 10$  GeV mass window in  $Pb - Pb$  collisions for two weeks of running time is 11000 with low background ( $\approx 4\%$ ). In the mass range  $20 \text{ GeV} \leq M(\mu^+\mu^-) \leq 50$  GeV the dominant contribution

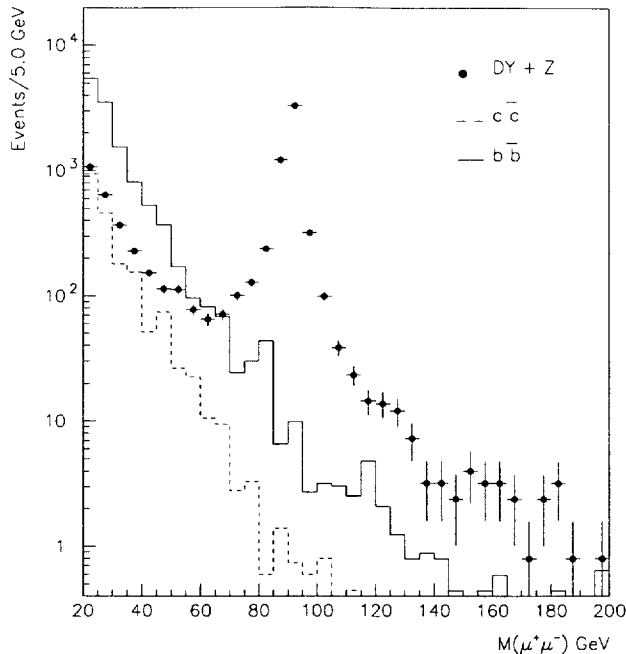


Figure 4: Invariant mass spectra of  $\mu^+\mu^-$  pairs for muons with  $P_T > 5$  GeV/c.

comes from  $b\bar{b}$  fragmentation (about 75%). The obtained number of dimuons from  $b\bar{b}$  semileptonic decays is about 27000. The Drell-Yan and  $c\bar{c}$  processes are giving nearly equal number of  $\mu^+\mu^-$  pairs in this range – 15% and 10% respectively. The contribution from  $t\bar{t}$  fragmentation and intermediate vector boson pair production is negligible at all masses. However the fraction of dimuons coming from  $c\bar{c}$  and  $b\bar{b}$  fragmentation can be significantly suppressed in this mass region if energy loss of heavy quarks is large.

## 5 Jet recognition and production rates in central $Pb - Pb$ collisions

The medium-induced radiative energy loss of high transverse momentum partons in heavy ion collisions provides important information about jet quenching and modification of the jet fragmentation function [14, 15]. Multiple scattering of high  $P_T$  partons on dense matter constituents should also lead to an enhanced acoplanarity and transverse momentum disbalance in two jet events [16, 17, 18, 19]. Since radiative energy loss and multiple scattering of the hard parton have a rather weak dependence on the initial parton energy, it is necessary to keep the energy of jets as low as possible. However, for central heavy ion collisions, it is difficult to extract low transverse energy jets due to large energy flow from the huge number of non-jet particles.

To study jet quenching process three different channels have been considered: QCD jet pair,  $Z(\rightarrow \mu^+\mu^-)+jet$  and  $\gamma+jet$  production. The advantage of the latter two channels is that initial transverse momentum of the parton is highly correlated to that of the  $Z(\gamma)$ , so the jet in this case can be considered as tagged, and the effects of its further evolution should be easier to determine, as opposed to the dijet case, where both jets are affected by the final state effects [20, 21].

The jet recognition efficiency and production rates were studied for QCD jet events only in the barrel part of the calorimeters ( $|\eta| \leq 1.5$ ). The modified UA1-type jet finding algorithm was used in  $\eta - \phi$  space. After finding a preliminary set of clusters, the merging/splitting procedure was applied for overlapping ones. Two clusters were merged into one jet if more than 75% of the transverse energy of the cluster with smaller  $E_T$  was contained in the overlap region. The direction and the energy of the new jet was then recalculated. If less than 75% of the  $E_T$  was contained in the overlap region, the clusters were split into two separate jets. The jet finding procedure was applied at three different stages of the simulation: i) at parton level; ii) at the particle level with all final state particles except neutrinos taken into account without momentum smearing; iii) at the calorimeter level for the same QCD jet event superimposed on the “thermal” particle background. Results from the first two steps were used for the

Table 3: Reconstruction efficiency  $\epsilon_1$ , contribution of “false” jets  $\epsilon_2$ , transverse energy resolution and production rates, for jets with different transverse energies.

$E_T \geq$ , GeV	$\epsilon_1$	$\epsilon_2$	$\sigma(E_T)/E_T$ , %	Rate
50	$0.94 \pm 0.03$	$0.120 \pm 0.030$	16.7	$1.7 \cdot 10^7$
100	$1.03 \pm 0.02$	$0.010 \pm 0.004$	11.6	$1.2 \cdot 10^6$
150	$0.98 \pm 0.02$	$0.004 \pm 0.003$	9.2	$2.1 \cdot 10^5$
200	$0.99 \pm 0.02$	$0.004 \pm 0.003$	8.6	$5.3 \cdot 10^4$

estimation of jet characteristics at the generator level and for the optimisation of jet finding algorithm for heavy ion collision simulation (the third step). In order to reduce the contribution from “false” jets originated from the fluctuations of the large transverse energy flow from non-jet particles, in central  $Pb - Pb$  collisions it is necessary to use a narrow cone radius  $R = \sqrt{(\Delta\eta)^2 + (\Delta\phi)^2}$  in the jet finding algorithm [22, 23]. In our analysis, the value of  $R = 0.3$  was used for cluster selection. It should be mentioned that in  $pp$  interactions about 80% of the jet transverse energy for high  $E_T$  jets ( $\approx 100$  GeV) is contained within this radius [24, 25].

For heavy ion collisions, before applying the jet finding algorithm, a simple iterative procedure was used to determine the average transverse energy of electromagnetic and hadronic calorimeter cells. The obtained value of  $\langle E_T^{cell} \rangle$ , multiplied by a factor  $\kappa$ , was subtracted from each cell. The value of  $\kappa$  was chosen to have a good matching between the generated and the reconstructed jet properties.

Table 3 presents the ratios of reconstructed to simulated jet numbers (reconstruction efficiency), relative contribution of “false” jets, transverse energy resolution and QCD jet production rates in central  $Pb - Pb$  collisions for two weeks of running time. The jet reconstruction efficiency is close to 100%. Contributions from “false” jets is  $12 \pm 3\%$  for  $E_T \geq 50$  GeV and becomes negligible for higher transverse energies. The resolution in jet transverse energy improves from 16.7% for  $E_T \geq 50$  GeV to 8.6% for  $E_T \geq 200$  GeV. For jet transverse energies lower than 50 GeV, background contribution increases rapidly and the energy resolution is worse. It should be mentioned that estimation of production rates does not take into account the trigger efficiency and data acquisition system capability, which will reduce the event rate by a factor of few depending on the trigger specifications in real running. Even in this case expected statistics will be enough to study high  $E_T$  jet production in  $Pb - Pb$  interactions as a function of the impact parameter of the collision and the transverse energy of jets.

Estimated statistics for  $Z(\rightarrow \mu^+ \mu^-)$ +jet and  $\gamma$ +jet production with transverse momentum of  $Z(\gamma)$  and jets greater than 50 GeV/c are 600 and 36500 events respectively in minimum bias  $Pb - Pb$  collisions for the same period of running time. However, for the  $\gamma$ +jet events background contribution from QCD jets with isolated  $\pi^0$  is very high (about 100%), which makes the use of  $\gamma$ +jet events difficult for the study of jet quenching process.

## 6 Conclusion

The possibility of the detection of dimuons and high transverse momentum jets in heavy ion collisions with CMS has been investigated.

The results of simulation shows that the acceptance for  $J/\psi$  state detection is mostly concentrated in the endcaps. The signal/background ratio for the full detector is very low 0.17 and increases considerably up to 1.8 if only the barrel part is used. However, in the barrel part only  $J/\psi$ 's with  $P_T > 5$  GeV/c can be detected. Detection of  $\Upsilon \rightarrow \mu^+ \mu^-$  decays can be performed with high acceptance in large pseudorapidity range  $|\eta| \leq 2.4$ . The ratio of  $S/B$  is 0.8 for the full detector and the expected number of detected  $\Upsilon$  decays in minimum bias  $Pb - Pb$  collisions is 55000 for two weeks of running time. These statistics will be enough to study  $\Upsilon$  state production as a function of its transverse momentum and centrality of the events. The obtained mass resolution, of the order of 40 MeV, is adequate to make clean separation between  $\Upsilon$  and  $\Upsilon'$  states. At the same time about 11000 events of  $Z \rightarrow \mu^+ \mu^-$  decays will be detected and can be used as benchmark process for understanding nuclear effects.

The jet recognition and production rates were studied in central  $Pb - Pb$  collisions. The jet recognition efficiency for  $E_T \geq 50$  GeV jets was found to be close to 100% with background  $12 \pm 3\%$ . The contribution of “false” jets can be further suppressed by requiring two jets to be approximately back-to-back in the transverse plane. The accuracy in the determination of the jet transverse energy is not perfect due to the large transverse energy flow of non-jet particles and its fluctuations. We find  $\sigma(E_T)/E_T = 16.7\%$  for jets with  $E_T \geq 50$  GeV, decreasing to 8.6% for 200 GeV jets. The jet energy smearing due to the resolution effects makes the study of jet quenching using only  $E_T$  distribution difficult. The multiple scattering and medium-induced radiative energy loss of the hard parton



should also lead to the potentially measurable modifications of the acoplanarity in dijet events and jet profiles. In order to simulate and study the possibility of such measurements, more precise theoretical calculations of these processes are necessary. Note also, that using  $\gamma$ +jet events for this study is questionable because of large QCD jet background. Expected statistics for  $Z(\rightarrow \mu^+\mu^-)$ +jet events in  $Pb - Pb$  collisions are rather low only about 600 events. However, for lighter ions this process looks very promising because of much higher luminosities.

It should be mentioned that presented production rates for  $Pb - Pb$  collisions are calculated for two weeks of running time at the average luminosity. If such luminosity has to be shared between two experiments, luminosity for each experiment will be about one fourth of the design one.

Finally, Monte-Carlo study shows that CMS detector is well adapted for the investigation of dimuon and high transverse momentum jet production in heavy ion collisions.

## References

- [1] H. Satz, in ECFA LHC Workshop Proceedings, CERN 90-10, ECFA 90-133 (1990), Vol. I, 188.
- [2] C. Singh, Phys. Rep. 236 (1993) 147.
- [3] H. Satz, Z. Phys. C 62 (1994) 683.
- [4] H.J. Specht, in ECFA LHC Workshop Proceedings, CERN 90-10, ECFA 90-133 (1990), Vol. II, 1236.
- [5] J.H. Harris and B. Müller, hep-ph/9602235.
- [6] CMS Technical Proposal, CERN/LHCC 94-38.
- [7] X.-N. Wang and M. Gyulassy, Phys. Rev. D 44 (1991) 3501.
- [8] T. Sjöstrand, Computer Physics Comm. 82 (1994) 74.
- [9] F. Antinori, ALICE/MC 93-09.
- [10] R. Gavai et al., CERN-TH.7526/94; BI-TP 63/94.
- [11] F. Abe et al., (CDF Collab.), Fermilab-Pub-95/271-E.
- [12] O. Kodolova and M. Bedjidian, CMS-TN/95-124.
- [13] M. Bedjidian, CMS Conference Report 1997/008.
- [14] M. Gyulassy and M. Plümer, Phys. Lett. B 243 (1990) 432; M. Thoma and M. Gyulassy, Nucl. Phys. B 351 (1991) 491; M. Plümer, M. Gyulassy and X.-N. Wang, Nucl. Phys. A 590 (1995) 511c.
- [15] R. Baier et al., Phys. Lett. B 345 (1997) 277; Nucl. Phys. B 478 (1996) 577; B 483 (1997) 291; B 484 (1997) 265.
- [16] D. A. Appel, Phys. Rev. D 33 (1986) 717.
- [17] J.-P. Blaizot and L. D. McLerran, Phys. Rev. D 34 (1986) 2739.
- [18] M. Rammerstorfer and U. Heinz, Phys. Rev. D 41 (1990) 306.
- [19] S. Gupta, Phys.Lett. B 347 (1995) 381.
- [20] V. Kartvelishvili, R. Kvatadze and R. Shanidze, Phys. Lett. B 356 (1995) 589.
- [21] X.-N. Wang, Z. Huang and I.Sarcevic, Phys. Rev. Lett. 77 (1996) 231; X.-N. Wang and Z. Huang, hep-ph/9701227.
- [22] R. Kvatadze and R. Shanidze, CMS TN/94-270.
- [23] N.A. Kruglov et al., CMS TN/96-084.
- [24] F. Abe et al., (CDF Collab.), Phys. Rev. Lett. 70 (1993) 713.
- [25] T.C. Heuring et al., (D0 Collab.), Fermilab-Conf-96/162-E.